# Identification of a β-Carboline Alkaloid from Chemoselectively Derived Vanilla Bean Extract and Its Prevention of Lipid Droplet Accumulation in Human Hepatocytes (HepG2)

**Dya Fita Dibwe [1], Nire Takeishi [2], Saki Oba [2], Akiko Sakurai [2], Toshihiro Sakurai [1], Takayuki Tsukui [3], Hitoshi Chiba [3] and Shu-Ping Hui [1,*]**

[1] Faculty of Health Sciences, Hokkaido University, Kita-12, Nishi-5, Kita-Ku, Sapporo 060-0812, Japan; dibwedf@hs.hokudai.ac.jp (D.F.D.); sakura@hs.hokudai.ac.jp (T.S.)
[2] Graduate School of Health Sciences, Hokkaido University, Kita-12, Nishi-5, Kita-Ku, Sapporo 060-0812, Japan; n10461991724nasukakstg@docomo.ne.jp (N.T.); saki.oba.h@gmail.com (S.O.); sakurai.akiko.p6@elms.hokudai.ac.jp (A.S.)
[3] Department of Nutrition, Sapporo University of Health Sciences, Nakanuma Nishi-4-3-1-15, Higashi-Ku, Sapporo 007-0894, Japan; tsukui@sapporo-hokeniryou-u.ac.jp (T.T.); chiba-h@sapporo-hokeniryou-u.ac.jp (H.C.)
* Correspondence: keino@hs.hokudai.ac.jp; Tel./Fax: +81-11-706-3693

**Table of contents:** **Supporting Information**

## 1. Materials and Methods

*Chemicals and instruments*

General Experimental Procedures: Nuclear magnetic resonance (NMR) spectra were recorded using a JEOL ECX400 Delta spectrometer with TMS as an internal standard; chemical shifts were expressed as *δ* values. An LTQ Orbitrap XL mass spectrometer (Thermo Fisher Scientific Inc., San Jose, CA, USA) was used for high-resolution electrospray ionization mass spectrometry (HR-ESI-MS) measurements. Low-resolution electrospray ionization mass spectrometry (LR-ESI-MS) spectra were recorded using an LXQ spectrometer (Thermo Fisher Scientific Inc., San Jose, CA, USA). Analytical thin-layer chromatography (TLC) was performed on pre-coated silica gel $60F_{254}$ and RP-$18F_{254}$ plates (0.25 or 0.50 mm, Merck KGaA, Darmstadt, Germany). Preparative TLC was performed on pre-coated silica gel 70 $PF_{254}$ plates (0.75 mm thickness; Wako Pure Chemical Industries, Ltd., Japan). Semi-preparative high-performance liquid chromatography (HPLC) separations were performed on a Shimadzu quaternary LC VL instrument with a UG 120 A column (250 × 10 mm; 5 μm I.D.). Methanol was purchased from Wako. High-glucose Dulbecco's Modified Eagle Medium (DMEM), Dulbecco's phosphate-buffered saline (DPBS), trypsin EDTA, fetal bovine serum (FBS), and penicillin-streptomycin (100 U/mL) were purchased from Gibco (Life Technologies, Carlsbad, CA, USA). Other materials used for cell culture were purchased from Corning (NY, USA). TLC silica gel 60G $F_{254}$ glass plates (20 × 20 cm) were obtained from Merck (Tokyo, Japan), and spots were visualized by spraying with 5% ethanolic $H_2SO_4$. $^{1}H$, $^{13}C$ NMR, Distortionless Enhancement by Polarization Transfer (DEPT), and two-dimensional (2D) NMR spectra were acquired using a 400 MHz JNM-ECX400P spectrometer (JOEL, Japan). The spectra were processed using JOEL software, and the chemical shift (*δ*) values were expressed in ppm. OA was purchased from Cayman Chemical (Ann Arbor, MI, USA), and absorbance was measured using ARVO-MX (Perkin Elmer, Waltham, MA, USA) as previously reported (15)

***2.*** *Liquid chromatography/mass spectrometry profiling of vanilla bean extract*

*LC-MS instrument conditions*

Samples of methanol BEs were separated using an Atlantis T3 C18 column (2.1×150 mm, 3 µm, 155 Waters, Milford, MA, USA) at a flow rate of 200 µL/min. LC gradient elution was performed using a mobile phase of 10 mM ammonium acetate solution, isopropanol, and methanol. The measurements were carried out in positive mode; the voltage of the MS capillary was 4.04 kV, flow rate of the sheath gas (nitrogen) was 50 psi, and auxiliary gas (nitrogen) was 20 psi. The high-resolution MS data were obtained in a scan range of *m/z* = 150–1100. MS/MS spectra were obtained by data-dependent acquisition using collision-induced dissociation (CID) in ion-trap mode for low-resolution masses. The raw data were processed using Xcalibur 2.2 (Thermo Fisher Scientific Inc., San Jose, CA, USA) as previously described (15).

***3.*** *Lipid metabolism-related gene expression.*

Gene expression analysis was performed using real-time PCR to investigate how the supplementation of compound **34** during LDA in HepG2 cells affects lipolysis and lipogenesis. HepG2 cells ($2.0\times10^5$/well) were seeded into 24-well plates (*n* = 6 per treatment). After 24 h, the cells were treated with PBS: 0.25 mM PBS for the OA-only group, 0.25 mM PBS for the OA plus group, and 125 and 250 µM PBS for the compound **34** group. After another 24 h, RNA extraction and complementary DNA synthesis were performed according to the manufacturer's instructions and as indicated previously. (15,54,55). The sequences of the primers used are shown in Table S1: adipose triglyceride lipase (*ATGL*), diacylglycerol O-acyltransferase 1 (*DGAT1*), sterol regulatory element-binding protein 1 (*SREBP1*), and glyceraldehyde-3-phosphate dehydrogenase (*GAPDH*). PCR was performed using a CFX 96 Real-Time PCR Detection System (Bio-Rad Laboratories Inc., Hercules, CA, USA) under the following conditions: 95 °C for 30 s, followed by 40 cycles at 95 °C for 5 s, 60 °C for 5 s,

and 72 °C for 10 s. All gene expression levels were analyzed using the ΔΔCt method and normalized to GAPDH. Data were represented as a relative expression based on the control group.

***4.*** *Lipid droplet accumulation inhibition assay*

LDAI activity was determined using an Oil Red O assay with 24-well plates ($n$ = 4 per treatment) based on a First, the staining of LDs in cultured hepatocytes was performed according to the manufacturer's instructions. Next, HepG2 cells ($1.5\times10^4$/well) were supplemented with 10% FBS, cultured, seeded into 35 mm dishes, and treated with the tested samples after 24 h. Oil Red O, a fat-soluble dye, is widely used for staining neutral lipids in LDs, as previously described (12). Next, quantification of LD inhibition was assessed for test compound **34** by comparing it to the untreated control group (+OA) and normalizing the LDA absorbance values (%) as previously reported (15). LD staining assay. Staining was performed as previously described with modifications (15).

***5.*** *Statistical analysis*

For gene expression analysis, mean values were compared using a one-way analysis of variance (ANOVA), followed by Tukey's multiple comparison test. Statistical analyses were performed using GraphPad Prism 8.0e (GraphPad Software Inc., La Jolla, CA, USA). Statistical significance was set at $p < 0.05$.

***6.*** *Complementary metabolite identification via DFF and,* $^1$*H-NMR analyses of selected bean extracts*

Natural products are usually synthesized as mixtures of structurally similar compounds instead of as a single compound. Because of their shared structural characteristics, numerous compounds of the same class are subject to similar MS/MS fragmentation and exhibit several identical product ions and/or neutral losses. The objective of DFF is to accurately detect all compounds of a specific class in a complex extract by filtering out non-targeted LC-MS/MS datasets for MS/MS spectra

that contain class-specific product ions and/or neutral losses (13, 27). The LC/MS profiling of the methanolic extract was presented as a 3D LC/MS plot with retention time and MS values (Figure S5-A). The LC/MS measurement and analysis of the vanilla BE revealed phenolic acid derivative metabolites (**1**).

It was possible to identify the phenolic derivative metabolites as major chemical constituents of the extract compared to the in-house standards. DFF is a straightforward and rapid strategy for detecting entire classes of compounds in a mixture of natural food products. DFF is especially relevant for the dereplication and discovery of natural product compounds. DFF was used for screening metabolites from LC-MS/MS datasets of BE8. The complementary results are 3D images and their DFF. The identified vanillin was further detected in the 3D LC-MS comparison of BE8 and vanillin standard and by using the DFF approach, as shown in the graph with the characteristic ion products and precursors from the LC-MS/MS analysis. As shown in the 3D plot in Figure 2A, vanillin (**1**) was found in the extract based on the retention time and MS/MS spectra of the authentic standard. The fragmentation behaviors of **1** were used for DFF analysis (Figure S5-B). The DFF results supported the GNPS and FooDB findings on this BE8 extract. Since vanillin has been previously reported to be effective in treating obesity, it would be interesting to investigate the effect of BE8 extract on NAFLD. Therefore, the LDAI activity of BE8 extract in HepG2 cells needs further investigation.

***7.** Identification of **34** using complementary* LC-MS/MS *diagnostic fragmentation filtering approach*

Natural products are usually synthesized as mixtures of structurally similar compounds instead of as a single compound. Because of their shared structural characteristics, numerous compounds of the same class are subject to similar MS/MS fragmentation and exhibit several identical product ions and/or neutral losses. The objective of DFF is to accurately detect all compounds of a specific class in a complex extract by filtering out non-targeted LC-MS/MS data sets for MS/MS spectra

that contain class-specific product ions and/or neutral losses (15, 32,33). DFF allows for the further discovery of all related natural products in a complex sample (13, 25, 27), but the main limitation of DFF approach is that the analyst must first define which product ions and/or neutral losses are specific to the targeted natural product class. Thus, in this study additionally to the identification of **34** by GNPS-MN analysis, DFF analysis of BE8 was performed as a complementary analysis for the identification of **34**. The proposed fragmentation results from synthetically prepared **34** was used for the DFF analysis. The LC–MS/MS analysis also resulted in the identification of **34** from the modified BE8. This result supported the identification of compound **34** by the GNPS-NM. Compound **34** was identified for the first time from the converted BE (*m*/*z* = 339.1339). The fragmentation pathway (Figure 4-A–C) demonstrates the possible fragments that defined the fragmentation characteristics of compound **34**. This fragmentation can be used for the analysis of the modified BE after heat treatment and acid modification.

The identification of **34** in the modified extract was also confirmed by using the complementary DFF approach, as shown in the 2D LC/MS representation plot (Figures 6). This evidence suggested that the LC/MS measurement and analysis of the modified extract revealed the presence of newly formed β-carboline alkaloid secondary metabolite **34** and the remaining L-tryptophan. It was possible to identify **34** as a newly formed chemical constituent in the modified BE by its comparison with the in-house β-carboline alkaloid synthetic standard. The identification of **34** was possible by using a complementary diagnostic fragmentation filtering approach (Figure S6). In Figure 6, the red dotted line represents the diagnostic product ions required to be considered a putative metabolite **34**. The blue dotted line represents the $[M+H]^+$ ions that are precursors of the β-carboline alkaloid **34**. Further research on analogous metabolites is required to fully explore the bioavailability of similar molecules in foods with a piperidine C-ring substituted with various moieties at C-1.

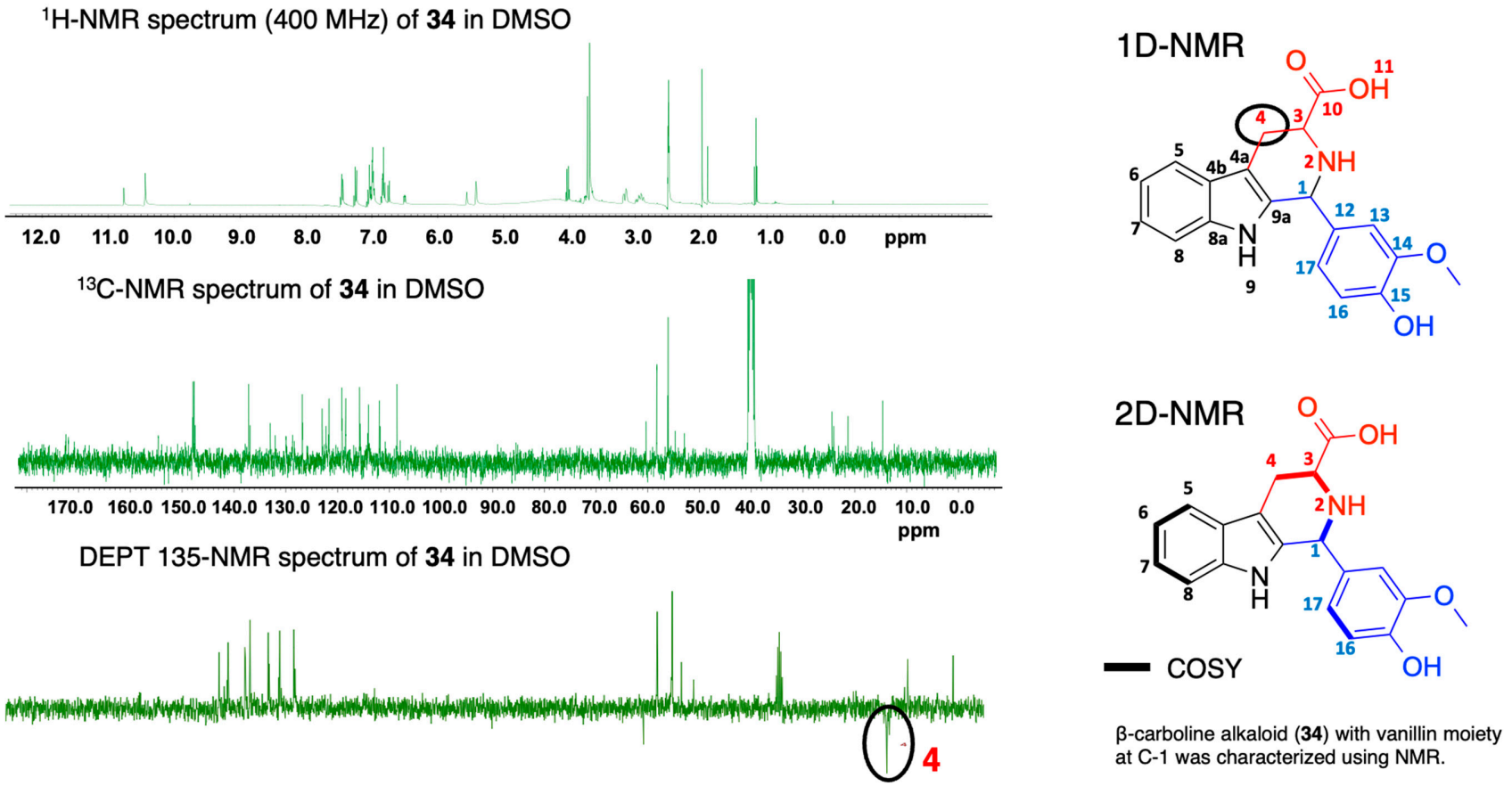


β-carboline alkaloid (**34**) with vanillin moiety at C-1 was characterized using NMR.

**Figure S1.** $^{1}$H NMR, $^{1}$H-$^{1}$H COSY, $^{13}$C NMR, and Dept 135 spectrum of β-carboline alkaloid (**34**) in $CDCl_3$.

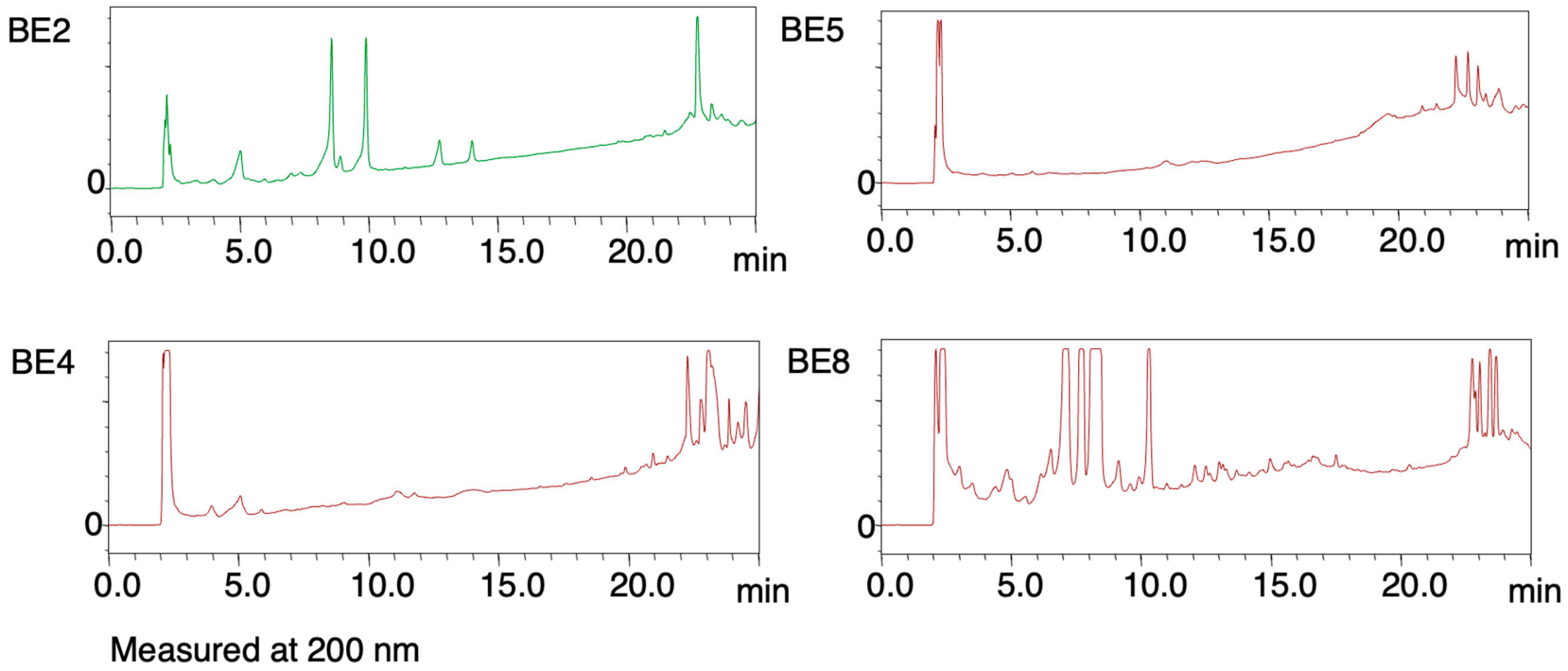


**Figure S2.** HPLC profiling of selected bean extracts: The comparison of BE2, BE4, BE5, and BE8 spectra.

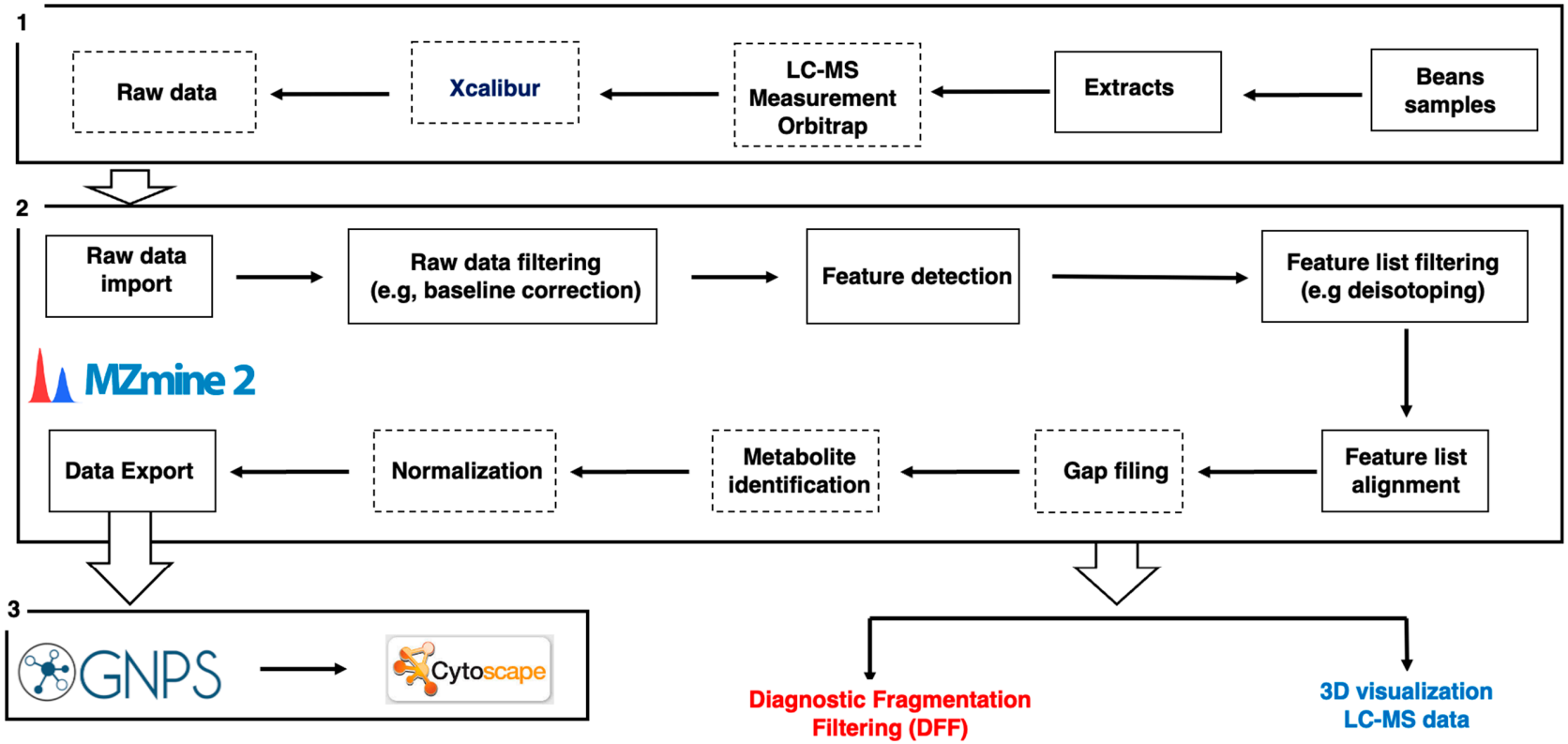


**Figure S3.** A schema of the general data processing workflow of LC-MS data.

| | BE2 (Sample 2) | | | | | BE4 (Sample 4) | | | | | BE5 (Sample 5) | | | | | BE8 (Sample 8) | | | |
|---|---|---|---|---|---|---|---|---|---|---|---|---|---|---|---|---|---|---|
| | RT | MS1(m/z) | MS2(m/z) | MS3(m/z) | | RT | MS1(m/z) | MS2(m/z) | MS3(m/z) | | RT | MS1(m/z) | MS2(m/z) | MS3(m/z) | | RT | MS1(m/z) | MS2(m/z) | MS3(m/z) |
| Peak 1 | 13.8808567 | 61.063961 | 61.086 | | Peak 1 | 13.9882783 | 79.0743332 | 60.9917 | | Peak 1 | 12.9643917 | 61.0639496 | 61.0828 | | Peak 1 | 12.4732167 | 61.0639458 | 61.2996 | |
| Peak 2 | 13.6150983 | 79.0743561 | 60.899 | | Peak 2 | 13.9882783 | 103.110535 | 60.9893 | | Peak 2 | 12.9643917 | 79.0743408 | 61.0057 | | Peak 2 | 12.4732167 | 79.0743408 | 60.8827 | |
| Peak 3 | 13.6150983 | 103.110565 | 60.9658 | | Peak 3 | 2.225215 | 104.113823 | 104.0125 | | Peak 3 | 13.736335 | 103.11055 | 60.9534 | | Peak 3 | 13.3664667 | 103.110542 | 60.8843 | |
| Peak 4 | 2.26449667 | 104.113853 | 60.0266 | | Peak 4 | 1.973025 | 130.084671 | 83.9342 | | Peak 4 | 2.25353833 | 104.113838 | 103.9469 | 59.8176 | Peak 4 | 13.4815067 | 135.09993 | 88.9332 | 69.026 |
| Peak 5 | 1.95884833 | 118.084915 | 100.0772 | 82.0911 | Peak 5 | 12.5871583 | 135.099915 | 88.9249 | 59.0415 | Peak 5 | 1.91789167 | 130.084686 | 83.9571 | 55.7687 | Peak 5 | 13.5380467 | 136.987152 | 108.8667 | 80.9309 |
| Peak 6 | 13.4163567 | 135.09996 | 88.8777 | 68.9882 | Peak 6 | 1.93799333 | 138.053238 | 137.9303 | | Peak 6 | 11.8570167 | 135.09993 | 88.9895 | | Peak 6 | 13.6813517 | 136.99585 | 108.8667 | 80.9309 |
| Peak 7 | 1.92302667 | 138.053299 | 138.0015 | | Peak 7 | 12.5871583 | 199.166946 | 111.1525 | 68.9211 | Peak 7 | 1.91789167 | 138.053284 | 137.9933 | 94.2974 | Peak 7 | 1.26978833 | 137.068016 | 108.8667 | 80.9309 |
| Peak 8 | 13.4553233 | 199.167007 | 111.1103 | 68.8976 | Peak 8 | 1.78979667 | 265.082336 | 135.9724 | 118.9279 | Peak 8 | 5.54421833 | 144.0821 | 97.9591 | 70.0993 | Peak 8 | 2.50825333 | 137.094315 | 108.8667 | 80.9309 |
| Peak 9 | 2.24256167 | 207.204376 | 103.9745 | 59.9237 | Peak 9 | 10.9211317 | 282.276001 | 265.21 | 247.3089 | Peak 9 | 1.91789167 | 144.100174 | 97.9591 | 70.0993 | Peak 9 | 12.1777017 | 137.094315 | 108.8667 | 80.9309 |
| Peak 10 | 10.9135883 | 282.276062 | 265.2249 | 247.1913 | Peak 10 | 12.5871583 | 287.218353 | 199.0962 | 111.0785 | Peak 10 | 1.98940333 | 144.100204 | 97.9591 | 70.0993 | Peak 10 | 3.84857667 | 137.09436 | 108.8667 | 80.9309 |
| Peak 11 | 13.4163567 | 287.218414 | 199.0778 | 111.0254 | Peak 11 | 10.35178 | 330.332886 | 312.3331 | 102.0276 | Peak 11 | 13.9460417 | 199.166962 | 111.209 | 68.9239 | Peak 11 | 2.47193333 | 152.045029 | 123.9966 | 94.9504 |
| Peak 12 | 1.86624 | 325.109375 | 288.8931 | 126.9222 | Peak 12 | 12.893235 | 338.337769 | 321.2432 | 303.2547 | Peak 12 | 1.80480333 | 265.082397 | 118.8564 | 72.869 | Peak 12 | 2.490035 | 153.05278 | 124.9418 | 92.8934 |
| Peak 13 | 10.42607 | 330.332947 | 312.3414 | 101.9587 | Peak 13 | 10.79307 | 356.348236 | 338.3278 | 102.0184 | Peak 13 | 10.9146033 | 282.276031 | 265.1783 | 247.2656 | Peak 13 | 7.695655 | 153.089088 | 124.9418 | 92.8934 |
| Peak 14 | 10.84576 | 356.348328 | 338.3103 | 101.9976 | Peak 14 | 12.5029767 | 391.279877 | 148.9346 | 120.9989 | Peak 14 | 11.8570167 | 287.218384 | 191.0818 | 110.9977 | Peak 14 | 5.49266333 | 153.089462 | 124.9418 | 92.8934 |
| Peak 15 | 1.88771167 | 360.146133 | 324.9626 | 288.9922 | | | | | | Peak 15 | 10.392585 | 330.332916 | 312.2337 | 102.0625 | Peak 15 | 8.411095 | 153.125488 | 124.9418 | 92.8934 |
| Peak 16 | 12.4952333 | 391.279999 | 148.9516 | 121.03 | | | | | | Peak 16 | 10.844945 | 356.348297 | 338.3009 | 102.0603 | Peak 16 | 2.490035 | 167.032074 | 151.975 | 124.0598 |
| | | | | | | | | | | Peak 17 | 1.86457 | 360.146118 | 324.9405 | 144.9609 | Peak 17 | 12.9475283 | 199.166962 | 111.1023 | 68.953 |
| | | | | | | | | | | Peak 18 | 12.5077717 | 391.279907 | 148.9234 | 120.8753 | Peak 18 | 10.9061183 | 282.276001 | 265.1479 | 247.2551 |
| | | | | | | | | | | | | | | | Peak 19 | 12.0883467 | 287.218384 | 199.0222 | 111.1176 |
| | | | | | | | | | | | | | | | Peak 20 | 11.7407283 | 323.254486 | 247.1617 | 121.0678 |
| | | | | | | | | | | | | | | | Peak 21 | 12.4732167 | 323.254486 | 247.1617 | 121.0678 |
| | | | | | | | | | | | | | | | Peak 22 | 10.3812133 | 330.332886 | 312.3016 | 102.0582 |
| | | | | | | | | | | | | | | | Peak 23 | 13.9496883 | 351.325363 | 275.2528 | 121.0859 |
| | | | | | | | | | | | | | | | Peak 24 | 10.9061183 | 356.348236 | 338.3432 | 101.9526 |
| | | | | | | | | | | | | | | | Peak 25 | 13.4815067 | 375.321442 | 357.3036 | 339.3403 |
| | | | | | | | | | | | | | | | Peak 26 | 14.000285 | 377.337036 | 319.3293 | 235.2205 |
| | | | | | | | | | | | | | | | Peak 27 | 11.661945 | 403.352509 | 385.2427 | 367.3871 |
| | | | | | | | | | | | | | | | Peak 28 | 12.964395 | 405.368073 | 387.3098 | 369.3398 |
| | | | | | | | | | | | | | | | Peak 29 | 12.4732167 | 431.383453 | 413.4841 | 395.2727 |
| | | | | | | | | | | | | | | | Peak 30 | 12.8286367 | 447.378082 | 389.322 | 371.2492 |

**Table S1.** LC-MS profiling using MZmine of bioactive bean extracts BE2, BE4, BE5, and BE8: Retention time (RT, min), $MS^1$, $MS^2$ and $MS^3$ (*m/z*).

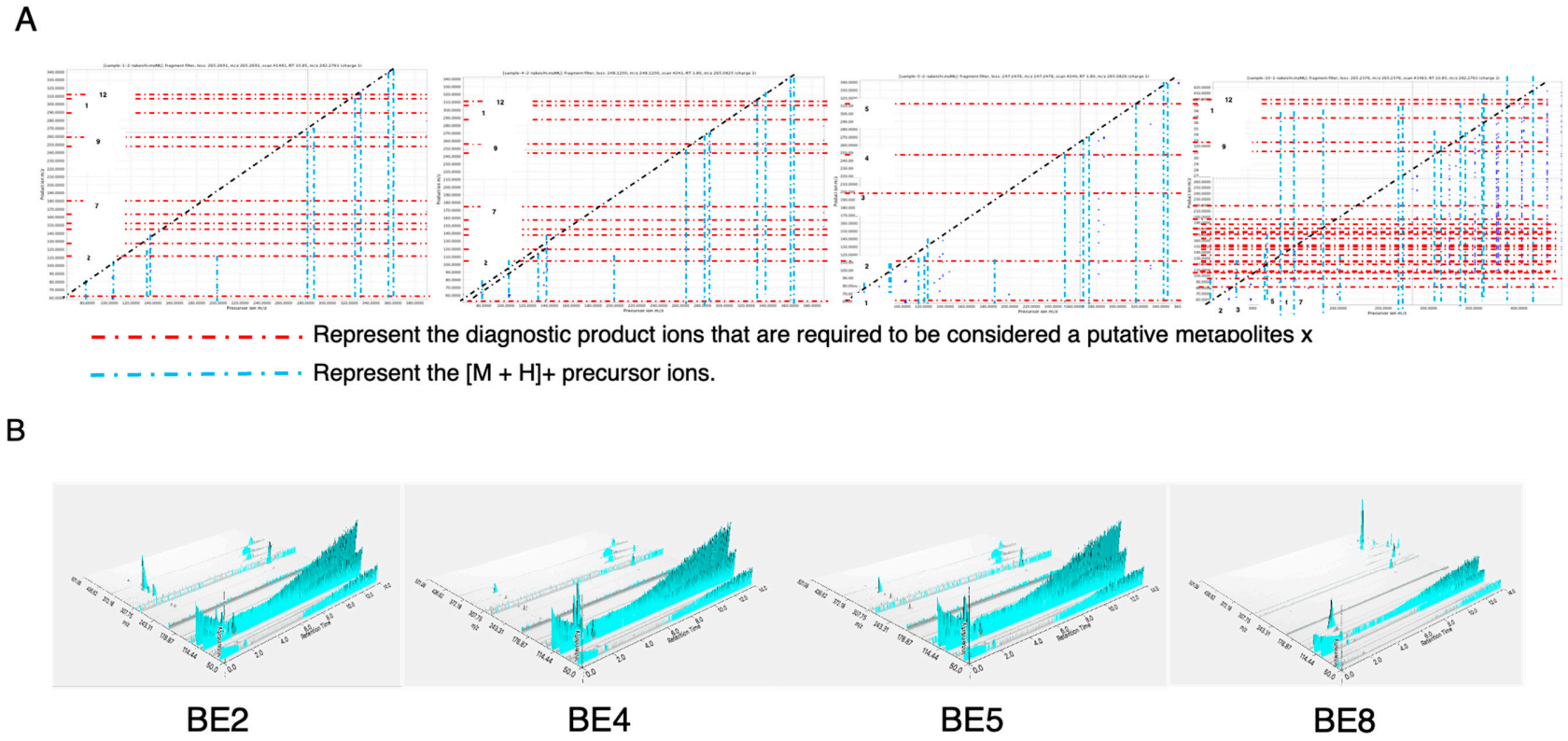


**Figure S4.** LC-MS profiling of bioactive bean extracts. (A) Diagnostic Fragmentation Filtering (DFF) plot for metabolites analysis. (B) 3D visualization of MS data.

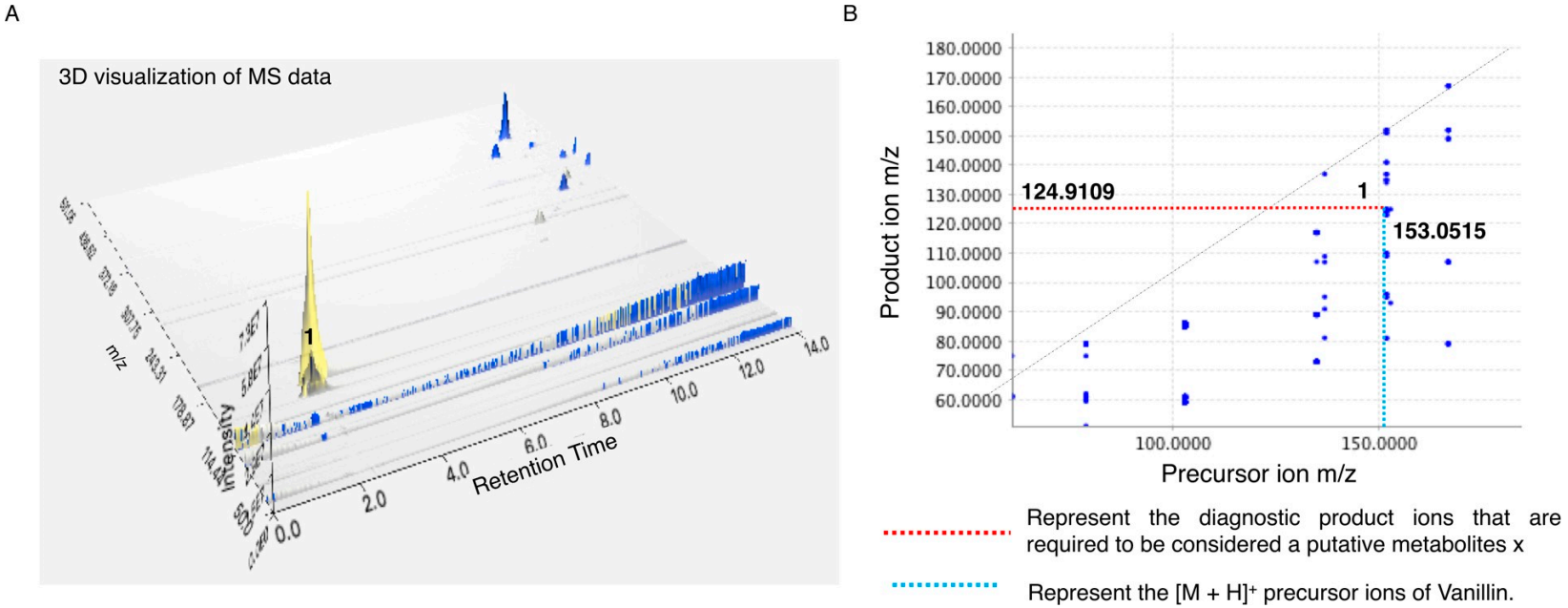


**Figure S5.** (A) Three-dimensional (3D) liquid chromatography/mass spectrometry (LC-MS) comparison of bean extract 8 (BE8) and vanillin. (B) Diagnostic fragmentation filtering (DFF) plot of the vanillin in BE8.

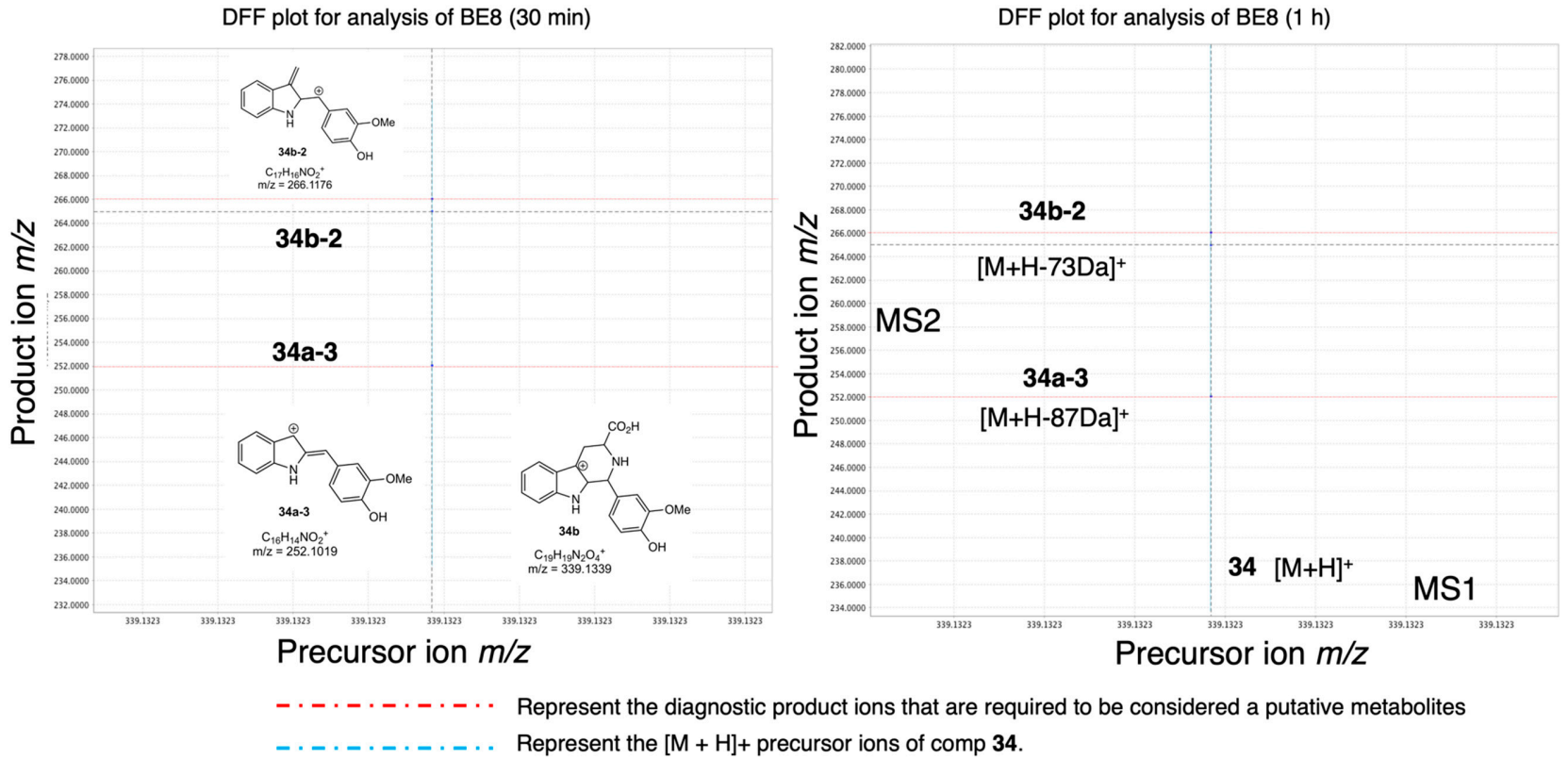


**Figure S6**. Diagnostic fragmentation filtering (DFF) identification of β-carboline alkaloid **34**: DFF analysis of **34** in modified vanilla BE -8 mixture after 30 min and 1 h of treatment.

**Table S2.** List of primers.

| Gene | Primer sequences (5' → 3') | | references: |
|---|---|---|---|
| ATGL | F: ACCAGCATCCAGTTCAACCT | R: ATCCCTGCTTGCACATCTCT | --> Adipose triglyceride lipase expression in human adipose tissue and muscle. Role in insulin resistance and response to training and pioglitazone |
| DGAT1 | F: TATTGCGGCCAATGTCTTTGC | R: CACTGGAGTGATAGACTCAACCA | --> https://www.hindawi.com/journals/omcl/2018/8515343/tab1/ |
| SREBP1 | F: CAGCCCACTTCATCAAGG | R: ACTGTTGCCAAGATGGTTCCG | --> https://www.hindawi.com/journals/omcl/2018/8515343/tab1/ |
| GAPDH | F: GAAGGTGAAGGTCGGAGTC | R: GAAGATGGTGATGGGATTTC | --> Bhullar, K.S., Shang, N., Kerek, E. et al. Mitofusion is required for MOTS-c induced GLUT4 translocation. Sci Rep 11, 14291 (2021). https://www.nature.com/articles/s41598-021-93735-2 |